Landsc Ecol
https://doi.org/10.1007/s10980-022-01553-2

RESEARCH ARTICLE

Fine-scale spatial heterogeneity shapes compensatory responses of a subalpine forest to severe bark beetle outbreak

Michele S. Buonanduci · Jenna E. Morris · Michelle C. Agne · Mike A. Battaglia · Brian J. Harvey

Received: 19 April 2022 / Accepted: 31 October 2022

Abstract

Context Growth releases of individuals that survive disturbances are important compensatory response mechanisms that contribute to ecological resilience. However, the role of fine-scale spatial heterogeneity in shaping compensatory growth responses is poorly understood for many broad-scale disturbances.

Objectives We quantified how fine-scale spatial structure affects individual and aggregate tree growth leading up to and following a severe mountain pine beetle (MPB; *Dendroctonus ponderosae*) outbreak. We asked: (1) How does individual tree growth vary with tree- and neighborhood-scale characteristics? (2) How do within-stand aggregate growth and overstory recruitment vary with neighborhood-scale characteristics?

Methods We used a spatially explicit long-term monitoring dataset of a subalpine lodgepole pine (*Pinus contorta* var. *latifolia*) forest (in Colorado, USA) in which every tree ≥ 5 cm diameter was measured and mapped prior to (1989, 2004) and following (2018) a severe MPB outbreak (2003–2011). We used spatial regression to characterize drivers of growth.

Results Overall, we found strong evidence for post-outbreak compensatory responses across spatial scales. Neighborhood characteristics shaped both individual and aggregate growth, with the magnitude of growth strongly mediated by pre-outbreak neighborhood structure and neighborhood mortality. Variation in tree-scale growth, combined with the spatial arrangement of surviving trees, resulted in highly variable emergent patterns of aggregate growth and recruitment.

Conclusion Our findings highlight the importance of fine-scale landscape configuration in shaping forest resilience. Quantifying compensatory responses in a spatially explicit framework at different scales is critical for modeling post-disturbance forest dynamics, which is increasingly important as climate warms and forest disturbance regimes change.

Supplementary Information The online version contains supplementary material available at https://doi.org/10.1007/s10980-022-01553-2.

M. S. Buonanduci · B. J. Harvey
Quantitative Ecology and Resource Management, University of Washington, Seattle, WA 98195, USA

M. S. Buonanduci (✉) · J. E. Morris · M. C. Agne · B. J. Harvey
School of Environmental and Forest Sciences, University of Washington, Seattle, WA 98195, USA
e-mail: mbuon@uw.edu

M. C. Agne
USDA Forest Service, Pacific Northwest Research Station, Olympia, WA 98512, USA

M. A. Battaglia
USDA Forest Service, Rocky Mountain Research Station, Fort Collins, CO 80526, USA

Published online: 23 November 2022

Keywords Growth release · Mountain pine beetle · Spatial model · Conifer forest · Rocky Mountains · Resilience

Introduction

Disturbances play an integral role in shaping the structure, function, composition, and development pathways of forests worldwide (Pickett and White 1985; Franklin et al. 2002). In North America, biotic disturbance agents (i.e., insects and pathogens) affect more forested area than wildfire annually (Dale et al. 2001; van Lierop et al. 2015). Eruptive species of native bark beetles (Curculionidae: Scolytinae) are among the most impactful disturbance agents; subcontinental-scale outbreaks can affect millions of hectares (ha) of forests over the course of several years to a decade, often resulting in > 80% mortality of host tree basal area (BA) within affected stands (Romme et al. 1986; Meddens et al. 2012; Simard et al. 2012; Jarvis and Kulakowski 2015).

Forests adapted to periodic disturbance exhibit some level of resilience, the capacity to tolerate disturbance without shifting to an alternative (e.g., non-forested) state (Holling 1973). The growth release of forests following bark beetle outbreak, driven by the responses of individual survivors to increased resource availability (e.g., light, water, nutrients), is an important compensatory response mechanism (Romme et al. 1986; Veblen et al. 1991) contributing to forest resilience. While seedling establishment is often the primary mechanism of resilience following stand-replacing disturbances such as wildfire, the growth release of previously established trees is a more important mechanism of resilience following stand-releasing disturbances such as bark beetle outbreaks (Hawkes et al. 2003; Astrup et al. 2008; Axelson et al. 2009; DeRose and Long 2010). Strong growth responses often occur for trees that were suppressed pre-outbreak, typically small-diameter trees and non-host or shade-tolerant species (Cole and Amman 1980; Hawkins et al. 2013). Growth releases are well documented as stand-level means, with dendroecological reconstructions of periods of growth release commonly used to detect the occurrence of past outbreaks (Alfaro et al. 2003; Jarvis and Kulakowski 2015). However, post-outbreak increases in resource availability and corresponding growth releases are unlikely to be uniform within a stand, highlighting the importance of within-stand spatial structure in shaping forest capacity for resilience (Cumming 2011).

Understanding mechanisms of forest resilience to disturbances is increasingly important as climate warms and disturbance activity accelerates worldwide (Turner 2010). The abundance, species composition, and spatial distribution of surviving trees are all biological legacies (*sensu* Franklin et al. 2000) that persist through bark beetle outbreaks and shape forest recovery (Nigh et al. 2010; Dhar and Hawkins 2011). Within-stand landscape pattern is itself an important biological legacy influencing the growth release of survivors (Wild et al. 2014), yet the role of fine-scale spatial pattern in shaping both individual and stand-level compensatory responses remains largely unexplored (Wild et al. 2014; Bače et al. 2015). Building an understanding of how spatial heterogeneity affects disturbance and resilience dynamics requires repeated, spatially explicit measurements (Bače et al. 2015; Lutz et al. 2014); thus, opportunities to build this understanding at the scale of individual trees are relatively rare. However, such insight is critical for characterizing how forest structure, demography, and function respond to disturbances such as bark beetle outbreaks (Dhar and Hawkins 2011; Pfeifer et al. 2011; Turner et al. 2013).

Here, we used a spatially explicit long-term monitoring dataset of a lodgepole pine (*Pinus contorta* var. *latifolia*) forest to characterize within-stand landscape drivers of individual and aggregate tree growth, both leading up to and following a severe mountain pine beetle (MPB; *Dendroctonus ponderosae*) outbreak. We studied three 2-ha plots in Fraser Experimental Forest (Colorado, USA) in which every tree ≥ 5 centimeters (cm) in diameter was censused, measured, and mapped leading up to (1989, 2004) and following (2018) a severe MPB outbreak (2003–2011) to address the following questions: (1) How do individual diameter growth rates of live trees vary with tree- and neighborhood-scale characteristics? (2) How do within-stand aggregate BA growth and overstory recruitment vary with neighborhood-scale characteristics? For each question, we identified tree- and neighborhood-scale characteristics expected to affect growth responses and tested hypothesized relationships (Table 1).

Table 1 Hypothesized relationships of individual and aggregate growth responses with tree- and neighborhood-scale characteristics

Scale	Characteristic	Hypothesized relationship	
		Direction	Justification
Question 1: Individual diameter growth			
Tree	Size	–	Growth rates decline as trees age and increase in size (Weiner and Thomas 2001), and growth release is expected to be greatest for small trees that were resource limited prior to the outbreak (Hawkins et al. 2013).
	Species	+/–	Late-seral, shade-tolerant species (subalpine fir and Engelmann spruce) expected to exhibit the greatest growth release relative to lodgepole pine (Hawkins et al. 2013); growth rates for Engelmann spruce expected to be greater than those for subalpine fir (Andrus et al. 2018).
Neighborhood	Density	–	Neighborhood density relates to increased resource competition (Contreras et al. 2011).
	Conspecifics	–	Conspecific neighboring trees expected to relate to increased resource competition (Chesson 2000; Getzin et al. 2006).
	Mortality	+	Neighborhood mortality relates to increased resource availability for survivors (Hawkins et al. 2013; Nigh et al. 2010).
	Topography	–	Convex microsites and steep slopes expected to relate to lower moisture availability.
Question 2: Within-stand aggregate basal area growth and overstory recruitment			
Neighborhood	Stem density	+	A greater number of trees corresponds to a greater potential for aggregate BA growth (Long and Vacchiano 2014) and overstory recruitment (Pukkala et al. 2009).
	Basal area	–	Aggregate BA growth expected to decrease with BA, following a size-related decline in stand growth (i.e., as individual tree growth rates decline with size) (Weiner and Thomas 2001). Recruitment also expected to decline with BA (Porté and Bartelink 2002; Pukkala et al. 2009).
	Late-seral proportion	+	Higher growth and establishment rates expected for late-seral, shade-tolerant species.
	Mortality	+	Neighborhood mortality expected to relate to increased growth responses of individual surviving trees.
	Topography	–	Convex microsites and steep slopes expected to relate to lower moisture availability

Methods

Study area

Fraser Experimental Forest (FEF) is located within the Arapaho-Roosevelt National Forest (Colorado, USA) in the Southern Rockies Ecoregion (Supplementary Material A, Fig. A1). The study stands are in subalpine forest composed of lodgepole pine seral to subalpine fir (*Abies lasiocarpa*) and Engelmann spruce (*Picea engelmannii*), with small quantities of quaking aspen (*Populus tremuloides*), gray alder (*Alnus incana*), Scouler's willow (*Salix scouleriana*), and Douglas-fir (*Pseudotsuga menziesii*) (Supplementary Material A, Fig. A2). Elevation ranges from 2790 to 2970 m. Stands are >300 years old, established following a stand-replacing fire in 1685 (Bradford et al. 2008). Climate is temperate and continental (Huckaby and Moir 1998) with mean monthly temperatures ranging from −8 degrees Celsius (°C) in January to 14 °C in July, a mean annual temperature of 3 °C, and a mean annual precipitation of 505 millimeters (30-year normals, 1991–2020; PRISM Climate Group 2021).

Between 2003 and 2010, a widespread, synchronous MPB outbreak occurred throughout the Southern Rockies, triggered by a severe drought in 2001–2002 (Chapman et al. 2012). Increasing MPB activity was noted in FEF in 2003 (Tishmack et al. 2005), reaching epidemic levels by 2006 (Hubbard et al. 2013) and subsiding by 2011 (Vorster et al. 2017). High rates of lodgepole pine mortality were

documented in FEF over the course of the outbreak, with MPB killing 90% of lodgepole pine trees over 30 cm in diameter at breast height (DBH) (Buonanduci et al. 2020; Rhoades et al. 2017).

Sampling design

Three 2-ha long-term monitoring plots were established in 1938 (Wilm and Dunford 1948) and surveyed periodically leading up to (1938, 1940, 1946, 1960, 1989, 2004) and following (2018) the MPB outbreak (Buonanduci et al. 2020). Prior to 2004, each survey consisted of a complete census of every living tree measuring at least 9 cm in DBH (measured 140 cm above the ground). In 2004 and 2018, the minimum DBH threshold was lowered to 5 cm. During each survey, DBH was recorded for each living tree and mortality cause was determined for all dead trees that were alive in the previous survey. In July and August 2018, we mapped all live and dead surveyed trees (n = 9357) within each plot to their horizontal coordinates and local elevation using FieldMap technology (Hédl et al. 2009; www.fieldmap.cz).

Growth metrics

The MPB outbreak in FEF occurred between approximately 2003 and 2011. While some mortality from MPB occurred prior to 2004 and was noted in the 2004 survey, 90% of MPB-caused tree mortality in the plots occurred after the 2004 survey (Buonanduci et al. 2020). Therefore, we used the 1989–2004 inter-survey period to quantify pre-outbreak growth and the 2004–2018 inter-survey period to quantify post-outbreak growth.

At the individual tree scale, we quantified the growth rate of trees between successive surveys as annualized diameter increment, calculated from successive DBH measurements (Table 2; Fig. 1a). We quantified growth release of individual trees as the difference in annualized diameter growth rate between the two growth periods (i.e., post-outbreak minus pre-outbreak growth rate) (Table 2; Fig. 1a). Rather than evaluating standardized diameter growth (i.e., growth relative to tree size), we accounted for potential growth-size relationships by including tree size as a covariate in our statistical modeling. Our individual tree scale analysis focused on lodgepole pine, Engelmann spruce, and subalpine fir, which accounted for > 99% of pre-outbreak live BA in the study plots. Growth rate estimates are below zero in some cases (6% and 2% of trees in pre- and post-outbreak periods, respectively; Table 2; Fig. 1a), which we attribute to measurement error from slight differences in positioning of diameter tapes among surveys.

At the within-stand scale, we quantified aggregate BA growth of live trees, a proxy for biomass accumulation, by rasterizing the point pattern of individual trees within each plot at a spatial resolution of 10 m. Within each 10 m raster cell and using only those trees that were alive and surveyed at both the beginning and end of each inter-survey period, we quantified BA growth as the total annualized change in live BA between successive surveys, calculated using successive DBH measurements (Table 2; Fig. 1b). This metric does not account for net decreases in total live BA due to mortality, which we incorporated as a covariate in this analysis. BA growth estimates are below zero in some cases due to measurement error in the field (1% and 0.2% of raster cells in pre- and post-outbreak periods, respectively; Table 2; Fig. 1b). We quantified aggregate BA growth release for each raster cell as the difference in BA growth between the two growth periods (i.e., post-outbreak minus pre-outbreak growth rate). Because the minimum survey diameter was lowered from 9 cm DBH in 1989 to 5 cm DBH in 2004, we only included trees ≥ 9 cm DBH when quantifying aggregate BA growth to allow for comparability of metrics between periods. For illustrative purposes, we also quantified net change in total live BA (i.e., BA growth minus BA mortality) (Fig. 2) but did not evaluate net change as a response variable in our modeling.

Finally, also at the within-stand scale, we quantified aggregate overstory recruitment, a measure of advance regeneration. We quantified overstory recruitment by counting the number of trees within each 10 m raster cell that grew to exceed the minimum survey diameter during the inter-survey period and were thus surveyed for the first time at the end of the inter-survey period (i.e., ingrowth density; Table 2; Fig. 1c). We quantified overstory recruitment

Table 2 Descriptive statistics for individual and aggregate growth responses[a] used in modeling

Metric	Growth period	n	Min	Max	Mean	Median
Individual diameter growth						
Lodgepole pine growth (cm/yr)	Pre-outbreak	2995	−0.11	0.68	0.06	0.05
	Post-outbreak	1401	−0.18	0.68	0.16	0.14
	Release	832	−0.59	0.48	0.09	0.08
Engelmann spruce growth (cm/yr)	Pre-outbreak	96	0.01	0.47	0.21	0.21
	Post-outbreak	177	−0.09	0.94	0.33	0.29
	Release	84	−0.48	0.50	0.10	0.07
Subalpine fir growth (cm/yr)	Pre-outbreak	160	0.01	0.65	0.21	0.20
	Post-outbreak	466	−0.17	0.96	0.28	0.26
	Release	146	−0.30	0.46	0.10	0.09
Within-stand aggregate growth						
Basal area growth of live trees ($m^2ha^{-1}yr^{-1}$)	Pre-outbreak[b]	505	−0.01	0.65	0.18	0.17
	Post-outbreak[b]	459	−0.01	0.75	0.22	0.20
	Release[b]	459	−0.36	0.58	0.03	0.02
Overstory recruitment (stems/ha)[c]	Pre-outbreak	506	0	500	55	0
	Post-outbreak[d]	505	0	1100	144	100
	Release[d]	505	−300	1100	90	100

[a]Response variables included here; see Supplementary Material B, Tables B1–B3 for predictor variables

[b]Datasets exclude raster cells with surviving basal area equal to zero, for which late-seral proportion could not be calculated

[c]Values presented here are scaled up to a per-ha basis. Unscaled 10 m raster cell counts were used for modeling

[d]Datasets exclude raster cells with initial basal area equal to zero, for which late-seral and mortality proportions could not be calculated

release for each raster cell as the difference in ingrowth density between the two growth periods (i.e., post-outbreak minus pre-outbreak). As with aggregate BA growth, we only included trees ≥ 9 cm DBH when quantifying overstory recruitment.

Potential predictors of individual tree growth

Tree size was quantified using DBH recorded at the start of each growth period (i.e., DBH recorded in 1989 was used as a predictor for pre-outbreak growth and DBH recorded in 2004 was used as a predictor for post-outbreak growth and growth release). Neighborhood density was quantified using a distance-dependent tree competition index, calculated as the sum of horizontal angles originating from each focal tree and spanning the DBH of each neighbor tree (Rouvinen and Kuuluvainen 1997; Contreras et al. 2011). We calculated neighborhood density within a 10 m radius as follows:

$$Neighborhood\ density = \sum_{i=1}^{n} arctan\left(\frac{DBH_i}{distance_i}\right)$$

where neighboring trees are indexed $i = 1, \ldots, n$; DBH_i is the DBH of neighboring tree i; and $distance_i$ is the distance between the center of the focal tree and the center of neighboring tree i. This index accounts for the number of neighboring trees, their proximity to the focal tree, and their size. We calculated neighborhood density using all neighboring trees, regardless of species. To quantify the relative density of conspecific trees, we calculated the proportion of the neighborhood density index contributed by the same species as the focal tree. To quantify neighborhood mortality, we calculated the proportion of the neighborhood density index that was killed (due to MPB or any other cause) during the growth period.

Fine-scale topography (i.e., elevation and slope) was quantified using a 1 m resolution digital elevation model developed from the local elevation of

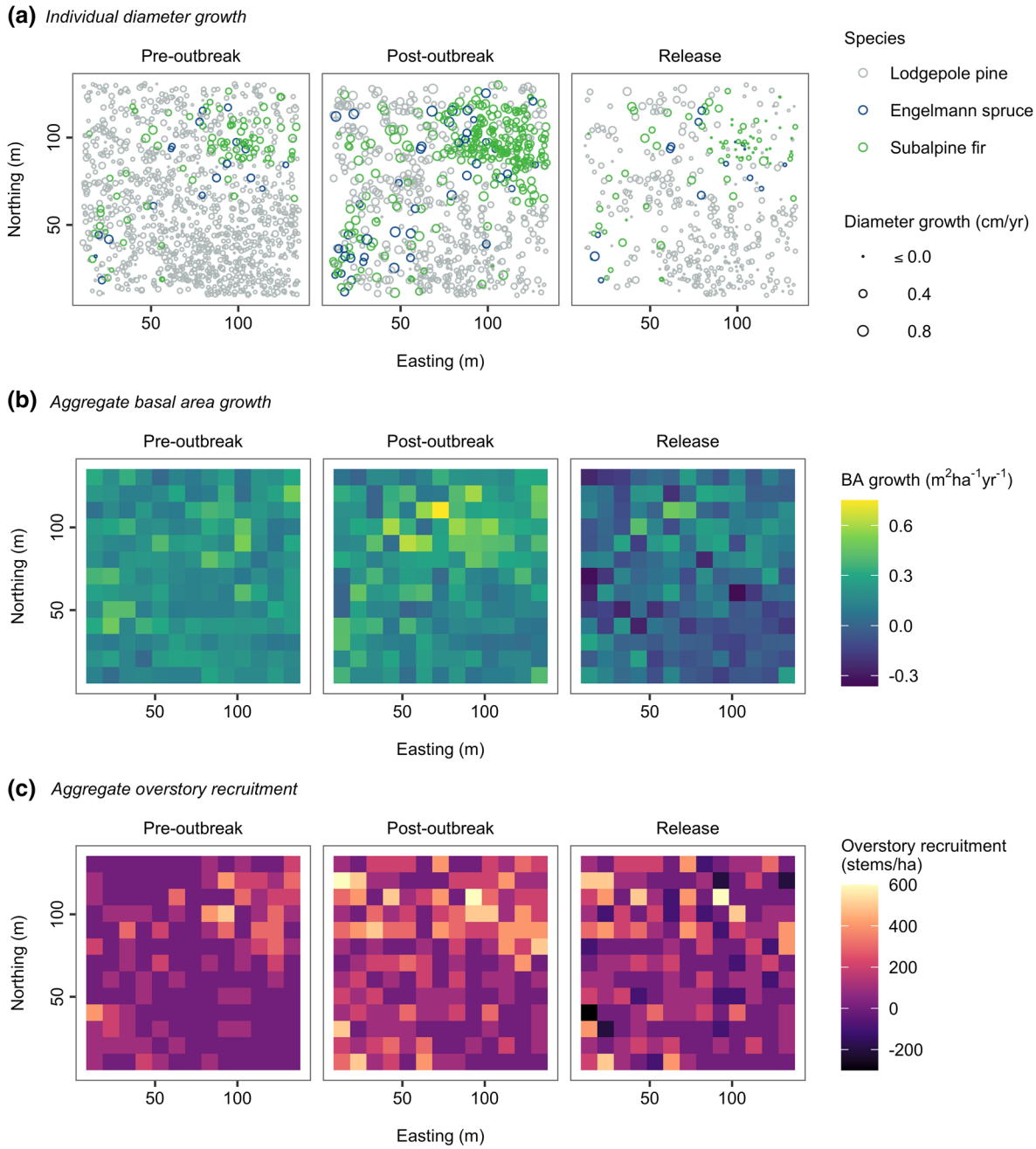

Fig. 1 Individual and aggregate tree growth responses in one plot (C3). **a** Individual diameter growth of live trees. **b** Aggregate basal area (BA) growth of live trees. **c** Aggregate overstory recruitment (ingrowth into ≥ 9 cm DBH size class). Cell size is 10 m and coordinates are relative to southwest corner of plot. To avoid boundary effects, trees located < 10 m from the edge of each plot were excluded from individual tree growth analyses, and raster cell centroids were positioned ≥ 10 m from the edge of each plot for aggregate tree growth analyses. Growth responses within all three plots included in Supplementary Material A

each individual tree measured in the field. We quantified local topographic position (i.e., topographic convexity versus concavity) using a topographic

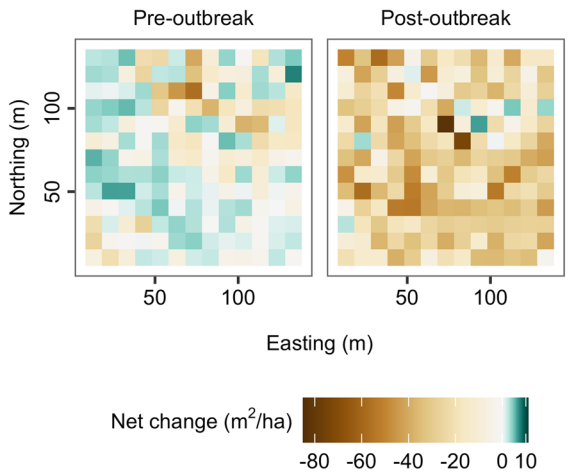

Fig. 2 Net change in total live basal area within one plot (C3). Cell size is 10 m and coordinates are relative to southwest corner of plot. Net changes in live basal area within all three plots included in Supplementary Material A

position index (Weiss 2001) calculated within a 10 m radius as follows:

$$Topographic\ position = z_0 - \bar{z}$$

where z_0 is the elevation of the cell containing the focal tree, and $\bar{z}$ is the average elevation around the focal cell within a predetermined radius. This index is positive when the focal tree is in a position higher than its neighbors on average (convex local topography) and negative when the focal tree is in a position lower than its neighbors on average (concave local topography).

Calculating neighborhood density and topographic position required specifying the neighborhood radius *a priori*. We chose a neighborhood radius of 10 m, comparable to radii used in tree competition studies conducted in lodgepole pine stands in British Columbia, Canada (Thorpe et al. 2010) and ponderosa pine (*Pinus ponderosa*) stands in Montana, USA (Woodall et al. 2003; Contreras et al. 2011). To avoid boundary effects, trees located < 10 m from the edge of each plot were excluded from analysis.

Potential predictors of within-stand aggregate growth and recruitment

Stem density and BA were quantified within each 10 m raster cell using live trees surveyed at the beginning of each growth period (i.e., live trees surveyed in 1989 were used for pre-outbreak growth metrics and live trees surveyed in 2004 were used for post-outbreak growth metrics and their release). Because only live trees that survived to the end of each growth period were used to calculate aggregate BA growth, only those same surviving trees were used to calculate stem density and BA for use as predictors of aggregate BA growth. Conversely, all live trees surveyed at the beginning of each growth period (regardless of survival) were used to calculate stem density and BA for use as predictors of overstory recruitment; this is because all initial live trees would potentially play a role, both leading up to and during the growth period, in the establishment of understory trees and their growth into the overstory (e.g., through seed production and competition).

We calculated late-seral proportion within each 10 m raster cell as the proportion of BA (i.e., surviving BA for growth and initial live BA for recruitment) composed of Engelmann spruce, subalpine fir, or any other late-seral species (i.e., those species present in the plots in smaller quantities). We calculated the mortality proportion within each 10 m raster cell as the proportion of initial live BA that was killed (due to MPB or any other causes) during the growth period. Topographic position and slope were calculated using the centroid of each raster cell as the focal location, using methods described above. To avoid boundary effects, raster cell centroids were positioned ≥ 10 m from the edge of each plot (i.e., a 5 m interior plot buffer was excluded from analysis).

Statistical analyses

We used Bayesian spatial regression models to make inference regarding the potential influence of covariates on each individual tree and aggregate growth metric. Growth responses for tree or raster cell $i (i = 1, \ldots, n)$ were modeled as random variables Y_i with mean μ_i measured at locations s_i. Models take the following form:

$$g(\mu_i) = \beta_0 + \sum_{k=1}^{K} \beta_k x_{ik} + a_i + \gamma_i$$

here, $g()$ is a link function, $x_{ik} (k = 1, \ldots, K)$ are covariates, a_i is a random effect of plot, and γ_i is a

spatial random effect modeled as a continuous Gaussian random field (GRF) measured at location s_i,

$$\gamma_i(s_i) \sim GRF(0, \Sigma)$$

We modeled the covariance matrix Σ using a Matérn covariance function parameterized by marginal standard deviation σ_γ and practical range r (distance at which correlation drops to approximately 0.1) (Lindgren et al. 2011).

Across growth periods, we found evidence for non-linear changes in aggregate BA growth with surviving stem density, which we modeled using a quadratic term for surviving stem density as a covariate. In the post-outbreak period (2004–2018), we found evidence for non-linear changes in individual tree growth rates with DBH for all three species, which we modeled using a smooth term on the DBH covariate. Thus, individual tree models in the post-outbreak period include a term u_l, which takes the form of a random walk of order one modeled at indices l of the binned DBH covariate:

$$u_l \sim Normal(u_{l-1}, \sigma_u^2)$$

Continuous growth responses (individual tree growth and aggregate BA growth), and the difference in aggregate overstory recruitment between time periods (which takes both positive and negative values), were modeled as Normal random variables with an identity link. Discrete pre- and post-outbreak overstory recruitment count responses were modeled as Poisson random variables with a log link.

Following methods described in Buonanduci et al. (2020), we used the Integrated Nested Laplace Approximation (INLA) and Stochastic Partial Differential Equation (SPDE) approaches to implement spatial models in a Bayesian framework (Lindgren et al. 2011; Blangiardo and Cameletti 2015) (Supplementary Material B, Fig. B1). To avoid spatial overfitting, we used penalized complexity priors for the marginal standard deviation and practical range of the GRF (Fuglstad et al. 2018). We used uninformative priors for all other parameters (Krainski et al. 2019). Both the INLA and SPDE approaches were implemented in R (R Core Team 2021) using the R-INLA package (www.r-inla.org).

We evaluated model fit via the conditional predictive ordinate (CPO; Pettit 1990), which is a *leave one out* cross-validation score. The sum of log CPO values is a useful summary of model fit, with larger sums indicating a better-fitting model (Blangiardo and Cameletti 2015). To enable comparison of the magnitude of coefficients within each model, we standardized all covariates within each dataset by subtracting their means and dividing by two times their standard deviations. A covariate or interaction term was considered an important predictor if the 95% credible interval for the coefficient did not include zero. We validated each model using standard regression diagnostics and tested for residual spatial autocorrelation using Moran's I (Cliff and Ord 1981). We conducted sensitivity analyses to confirm that varying the spatial resolution of individual tree growth covariates (i.e., using 5, 10, or 15 m radii to quantify neighborhood characteristics) or aggregate growth response variables (i.e., using 5, 10, or 15 m raster cells to quantify aggregate metrics) would not qualitatively change the results and conclusions (Supplementary Material B, Figs. B2–3).

When modeling individual tree growth responses, we first fit a single model for each growth period with species included as the only fixed effect to test for overall differences in species-specific magnitudes of growth. We then fit species-specific models for each growth response, including all potential covariates. Because we expected some covariate effects might vary with tree size, we considered interaction terms between DBH and all other covariates. To limit the overall number of statistical tests, we added interaction terms to each model only if they were important predictors (i.e., 95% credible interval for the interaction term did not include zero) *and* they improved model fit (i.e., increased the sum of log CPO values).

Results

Heterogeneity in tree- and neighborhood-scale characteristics

Within stands and across growth periods, tree- and neighborhood-scale characteristics varied widely (Supplementary Material B, Tables B1 – B3). Neighborhood density and composition, for example, were highly variable within stands both pre- and post-outbreak, with live BA ranging from 0.6 to 115.9 m^2/ha and late-seral proportion ranging from 0.0 to 1.0 (Supplementary Material B, Tables B2 – B3).

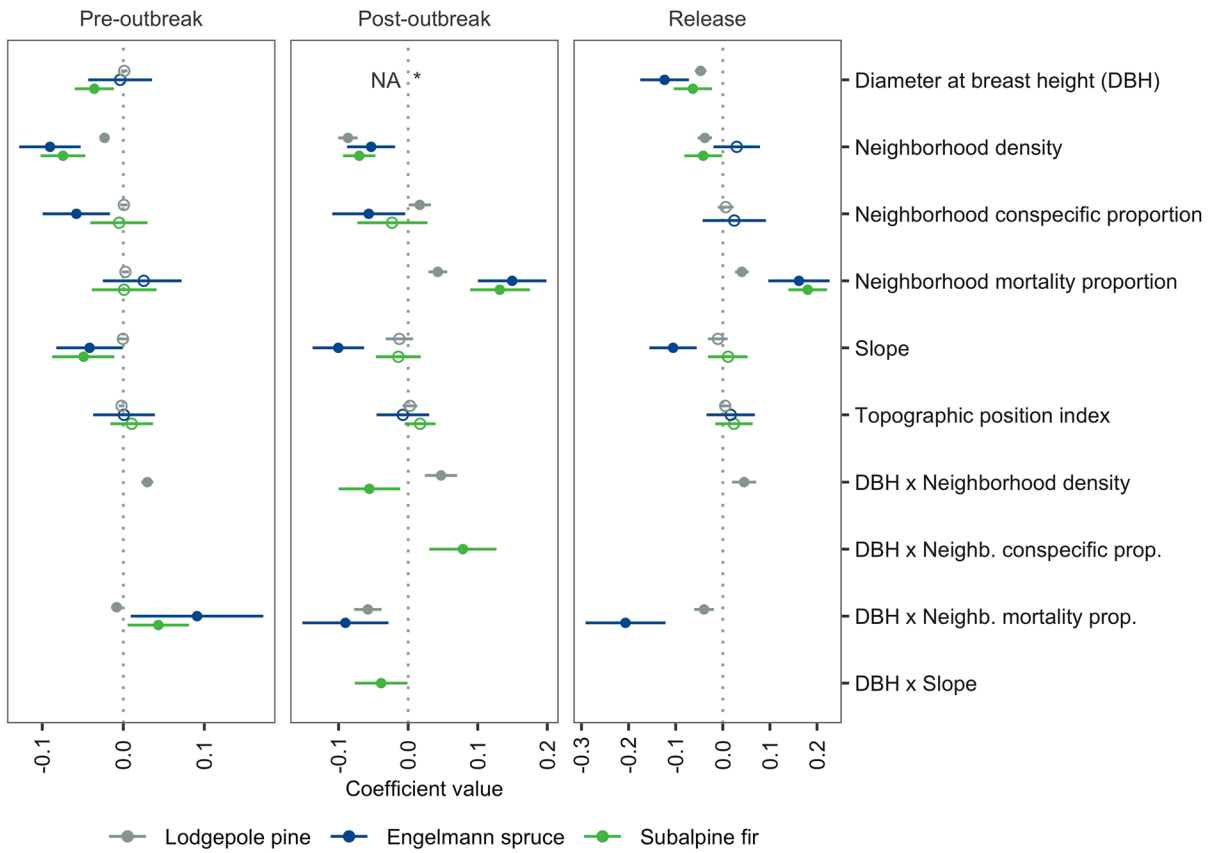

Fig. 3 Effect of covariates on individual tree diameter growth responses. Here and in Fig. 5, dots represent the medians of the posteriors and horizontal lines represent 95% credible intervals. Closed circles represent statistically important predictors, and open circles represent predictors that are not statistically important. The effects for each predictor are per 2 SD within each growth period- and species-specific dataset. Blank spaces indicate covariates not evaluated in a particular model. *See Supplementary Material B, Fig. B5 for non-linear effect of DBH in the post-outbreak period

Neighborhood mortality proportion was relatively low on average in the pre-outbreak period (mean ranging from 0.1 to 0.2 across datasets) compared to the post-outbreak period (mean ranging from 0.5 to 0.8 across datasets); however, a wide range in neighborhood mortality proportion was observed within plots across both periods (minimum ranging from 0.0 to 0.07 and maximum ranging from 0.6 to 1.0 across datasets; Supplementary Material B, Tables B1–B3).

Individual tree diameter growth

Within each growth period (i.e., pre-outbreak, post-outbreak, and release), diameter growth responses of late-seral, shade-tolerant species (i.e., Engelmann spruce and subalpine fir) were greater than those of lodgepole pine (Table 2; Fig. 1a), with estimated mean growth responses being greatest for Engelmann spruce, followed by subalpine fir and then lodgepole pine (based on regression models with species as the only fixed effect; Supplementary Material B, Table B4). Estimated mean growth releases for each species were greater than zero (based on intercept-only regression models; Supplementary Material B, Table B5). The direction and magnitude of effects of covariates varied by growth period and species (Fig. 3; Supplementary Material B, Table B6).

Pre-outbreak growth (1989–2004)

In the pre-outbreak period, neighborhood density had a strong effect on growth rates across species, with lodgepole pine, Engelmann spruce, and subalpine fir growth rates all decreasing with neighborhood density

(Fig. 3). For lodgepole pine, the negative effect of neighborhood density lessened with increasing DBH (Fig. 3), suggesting that growth rates of small lodgepole pine decreased more sharply with neighborhood density than growth rates of large lodgepole pine. Interaction terms of DBH and neighborhood mortality suggest growth rates varied marginally with neighborhood mortality, though the direction of effects differed both with tree size and by species (Fig. 3). Additional marginal effects of neighborhood conspecifics and slope steepness were observed for Engelmann spruce, and additional marginal effects of DBH and slope steepness were observed for subalpine fir (Fig. 3).

Post-outbreak growth (2004–2018)

In the post-outbreak period, neighborhood density, neighborhood mortality, and DBH had strong effects on growth rates across species, with lodgepole pine, Engelmann spruce, and subalpine fir growth rates all decreasing with neighborhood density and increasing with neighborhood mortality (Fig. 3). Growth rates of all species increased with DBH up to ~10–20 cm DBH, beyond which growth rates decreased with further increases in DBH (Supplementary Material B, Fig. B5). Furthermore, effects of neighborhood-scale characteristics varied with tree size and among species. For lodgepole pine, growth rates of small trees decreased more sharply with neighborhood density than growth rates of large trees; conversely, for subalpine fir, growth rates of large trees decreased more sharply with neighborhood density than growth rates of small trees (Fig. 3). For both lodgepole pine and Engelmann spruce, the positive effect of neighborhood mortality lessened with greater DBH (Fig. 3). Additional marginal effects of neighborhood conspecifics were observed for all species, and additional marginal effects of slope steepness were observed for Engelmann spruce and subalpine fir, though the direction of effects varied (Fig. 3).

Growth release

For all three tree species, growth releases were strongly related to DBH and neighborhood mortality, with growth releases being greatest for small trees and decreasing with greater DBH (Figs. 3 and 4). Growth releases of all species increased with neighborhood mortality, and for lodgepole pine and Engelmann spruce, growth releases of small trees increased more sharply with neighborhood mortality than growth releases of large trees (Figs. 3 and 4). Growth releases of lodgepole pine and subalpine fir decreased with neighborhood density, though the effect of neighborhood density lessened with greater DBH for lodgepole pine (Figs. 3 and 4). An additional marginal effect of slope steepness was observed for Engelmann spruce. While we could not evaluate the effect of neighborhood conspecifics for subalpine fir growth releases due to issues of

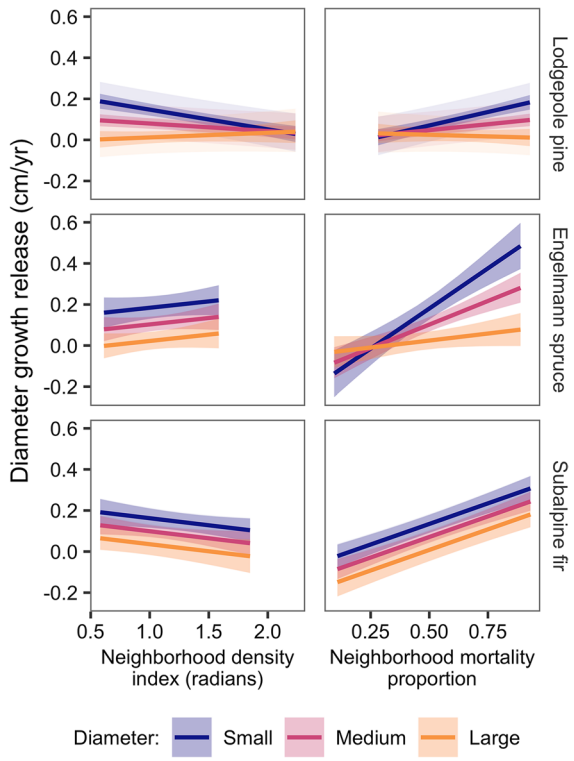

Fig. 4 Change in relationship between covariates (x-axis) and predicted individual diameter growth release (y-axis) across gradients of tree diameter. Small, medium, and large diameters specified as 10, 20, and 30 cm respectively for lodgepole pine and 10, 25, and 40 cm respectively for Engelmann spruce and subalpine fir. Solid lines represent posterior medians, dark shading represents 95% credible intervals for predictions at one location, and light shading represents variability in 95% credible intervals for predictions across locations (i.e., variability modeled by the spatial GRF; not visible for Engelmann spruce or subalpine fir due to low level of variation attributed to spatial GRF in these models). Predictions consider each combination of covariates in isolation, holding all other covariates at zero (i.e., their average values)

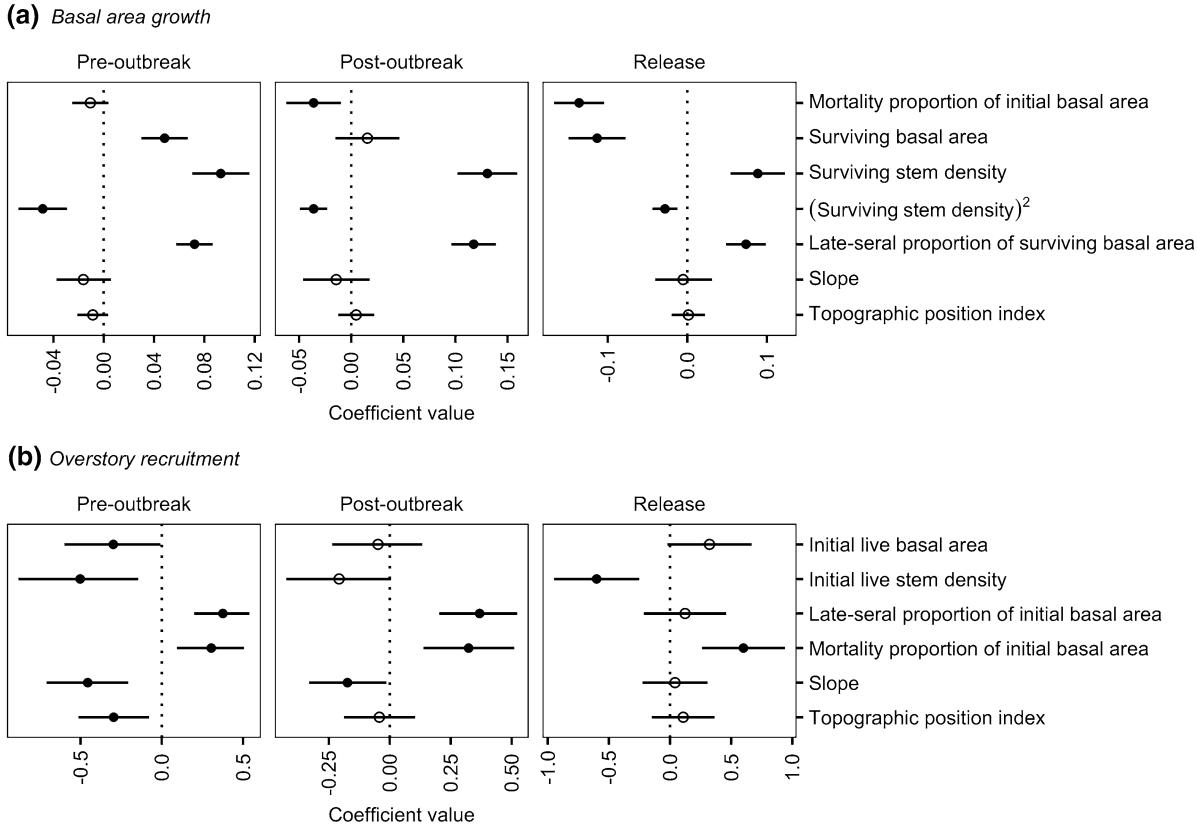

Fig. 5 Effect of covariates on aggregate growth responses. **a** Aggregate basal area growth of live trees. **b** Aggregate overstory recruitment. Symbols are described in Fig. 3

collinearity, we did not detect an effect of neighborhood conspecifics on growth releases of the other species.

Within-stand net change in live basal area

Net changes in total live BA (i.e., BA growth minus mortality) were largely negative in the post-outbreak period (Fig. 2). Within plots, net changes in live BA over the pre-outbreak period ranged from −57.3 to 9.8 m^2/ha (mean = −3.8 m^2/ha, median = 0.2 m^2/ha). Over the post-outbreak period, net changes in live BA ranged from −86.0 to 7.1 m^2/ha (mean = −26.5 m^2/ha, median = −27.0 m^2/ha; Fig. 2).

Within-stand aggregate basal area growth

Aggregate BA growth varied widely across the within-stand landscape and between growth periods (Table 2; Fig. 1b). BA growth releases also varied widely across the within-stand landscape (Table 3; Fig. 1b), though the mean was not statistically different from zero (based on an intercept-only regression model; Supplementary Material B, Table B7).

The direction and magnitude of factors associated with within-stand aggregate BA growth varied by growth period (Fig. 5a; Supplementary Material B, Table B8). Pre-outbreak, BA growth rates were unrelated to mortality proportion (Fig. 5a). Pre-outbreak BA growth rates increased with surviving BA (i.e., BA of live trees that survived the growth period), increased then plateaued with surviving stem density (positive main effect and negative quadratic term), and increased with the proportion of surviving BA composed of late-seral species (Fig. 5a). Post-outbreak, BA growth rates decreased with mortality proportion and were unrelated to surviving BA (Fig. 5a). Post-outbreak BA growth rates increased then plateaued with surviving stem density (positive main effect and negative quadratic term) and increased

with the proportion of surviving BA composed of late-seral species (Fig. 5a). BA growth releases decreased with mortality proportion and surviving BA, increased then plateaued with surviving stem density, and increased with the proportion of surviving BA composed of late-seral species (Fig. 5a).

Within-stand aggregate overstory recruitment

Overstory recruitment density varied widely across the within-stand landscape and between growth periods (Table 2; Fig. 1c). On average, recruitment release was statistically greater than zero (based on an intercept-only regression model; Supplementary Material B, Table B9). Pre- and post-outbreak, overstory recruitment was predominantly lodgepole pine (49% and 56% of stems), followed by subalpine fir (34% and 33% of stems) and Engelmann spruce (13% and 9% of stems), with species-specific spatial patterns generally following patterns of the pre-outbreak canopy (Supplementary Material A, Fig. A6).

The factors associated with within-stand aggregate overstory recruitment remained relatively consistent across time periods, though the relative magnitude of effects changed (Fig. 5b; Supplementary Material B, Table B10). Pre-outbreak, overstory recruitment decreased with initial live BA (i.e., BA of trees alive at the beginning of the growth period), initial live stem density, slope, and topographic position (i.e., convexity) (Fig. 5b). Pre-outbreak overstory recruitment increased with both the proportion of BA composed of late-seral species as well as with mortality proportion (Fig. 5b). Post-outbreak, overstory recruitment also decreased with slope and increased with both the proportion of BA composed of late-seral species and with mortality proportion (Fig. 5b). Overstory recruitment releases decreased with initial live stem density and increased with mortality proportion (Fig. 5b).

Discussion

Using a unique spatially explicit long-term monitoring dataset, our study highlights mechanisms of forest recovery following bark beetle outbreak and demonstrates the importance of spatial heterogeneity in directing ecosystem response to disturbance. Overall, we found strong evidence for compensatory responses of forests at multiple scales following the outbreak, with increases in individual tree diameter growth and overstory recruitment density, as well as stability in aggregate BA growth of live trees despite outbreak-induced decreases in live BA. Neighborhood characteristics shaped both individual and aggregate growth responses following severe MPB outbreak, with the magnitude of responses strongly mediated by pre-outbreak neighborhood structure and neighborhood mortality. Individual tree growth responses varied widely with tree- and neighborhood-scale characteristics; this tree-scale variation, combined with the spatial arrangement of survivors, resulted in highly variable emergent patterns of within-stand aggregate BA growth and overstory recruitment. Our findings have important implications for understanding the role of spatial heterogeneity in shaping post-disturbance forest dynamics and associated ecosystem services (Turner et al. 2013).

Strong post-outbreak compensatory responses occurred across spatial scales

Following the severe mortality caused by the MPB outbreak, we found strong compensatory responses in both individual and aggregate within-stand growth, demonstrating an important mechanism of forest resilience at multiple spatial scales. As expected, diameter growth rates of individual surviving trees increased on average for all species, and overstory recruitment density increased as growth releases of small-diameter trees enabled a greater number of understory trees to grow into the overstory. Rates of recovery can be variable following bark beetle outbreak; some stands recover relatively quickly (e.g., within several decades), while others are much slower to return to pre-outbreak BA and density (Griesbauer and Green 2006). Further research would be needed to determine the rate of recovery in our study stands, particularly in the context of a warming and drying climate. However, our finding of accelerated recruitment of overstory trees suggests that responses of growth to resource release will eventually compensate for the reduction in overstory BA and stem density resulting from the outbreak.

Compensatory responses of surviving trees were sufficient to maintain continuity in rates of biomass accumulation across stands, which has important implications for carbon sequestration both leading

up to and following bark beetle outbreaks. Aggregate BA growth varied widely with both stand structure and growth responses of individual trees, implying similarly wide spatial variation in carbon fluxes at the within-stand scale (Pfeifer et al. 2011). Despite net changes in live BA being largely negative in the post-outbreak period (i.e., fewer live trees contributing to aggregate BA growth), aggregate BA growth did not change on average from pre- to post-outbreak, suggesting that though spatially variable within stands, there was overall stability in rates of biomass accumulation when scaled up to the stand. Our results are consistent with findings elsewhere in the Southern Rockies, where stability in biomass accumulation has been found despite increases in mortality at aggregate stand scales (Chai et al. 2019), and compensatory responses following beetle outbreaks is strong among stands across the region (Rodman et al. 2022). Our results are also consistent with findings that net uptake of atmospheric carbon within stands can recover within just a few years of MPB outbreak (Brown et al. 2012). This stability in within-stand productivity and carbon uptake despite substantial losses of live biomass is an important dimension of forest resilience (Turner et al. 2013; Davis et al. 2022), one that is facilitated by rapid redistribution of productivity within a stand following stand-releasing disturbance (Romme et al. 1986).

Pre-outbreak neighborhood structure and neighborhood mortality drive compensatory growth responses

Consistent and strong effects of neighborhood structure on tree growth in our study highlight the importance of resource competition, an inherently spatial process, in driving compensatory responses to disturbance across scales. Prior to and following the outbreak, individual tree diameter growth rates and aggregate overstory recruitment density decreased with neighborhood density (i.e., neighborhood competition). Conversely, aggregate BA growth increased with surviving neighborhood density (since a higher number of surviving trees translates to a higher potential for aggregate growth). However, this positive relationship plateaued in high-density neighborhoods as competition imposed limits on further increases in aggregate growth. The differing forms of these relationships reflect the similar role yet differing signature of neighborhood density in shaping individual- versus aggregate-level growth rates (Long and Vacchiano 2014). Our results illustrate the inherent tradeoff between individual and aggregate growth within a stand (Long et al. 2004) and demonstrate the importance of competition for resources (i.e., light, water, nutrients) as a mechanism limiting tree growth (Craine and Dybzinski 2013) across spatial scales.

Following the outbreak, neighborhood mortality strongly drove compensatory growth responses, particularly for small-diameter trees. Small-diameter trees responded more strongly to resources released by overstory mortality compared to large-diameter trees, supporting similar tree-scale findings elsewhere (Cole and Amman 1980; Veblen et al. 1991; Hawkins et al. 2013). While small-diameter trees generally have a greater capacity for diameter growth compared to large-diameter trees, their growth is also more likely to be suppressed via competition for light and belowground resources when growing in the mid- to lower-canopy of uneven-aged stands (Oliver and Larson 1996; Caspersen et al. 2011). When mortality occurs nearby, particularly severe overstory mortality that increases light availability, small-diameter trees therefore demonstrate the greatest growth release (Romme et al. 1986). At the within-stand scale, our finding that overstory recruitment density increased with neighborhood mortality follows from the strong growth responses of small-diameter trees, which effectively accelerated the growth of understory trees into the overstory. Our findings highlight how the interaction of tree- and neighborhood-scale characteristics can result in strong compensatory growth responses following stand-releasing disturbances.

While neighborhood mortality strongly shaped growth responses following the outbreak, growth responses prior to the outbreak were less consistently affected by nearby mortality. Pre-outbreak growth rates of some trees increased with neighborhood mortality while others decreased; aggregate BA growth was unrelated to mortality, whereas aggregate overstory recruitment density increased with mortality. Following low-level disturbance or mortality resulting from gradual decline, growth releases of nearby trees may be mixed or modest (Thompson et al. 2007). Mortality levels were relatively low during the pre-outbreak period, which likely explains why growth responses to neighborhood mortality were mixed. In the absence of severe and punctuated

disturbance (i.e., in the context of background mortality), our results suggest compensatory responses to neighborhood mortality may be inconsistent or difficult to detect.

Across a range of mortality levels, our findings suggest a persistent legacy of pre-outbreak neighborhood structure on post-outbreak growth responses. After accounting for neighborhood mortality, growth releases of individual lodgepole pine and subalpine fir, as well as releases of aggregate overstory recruitment, decreased with initial neighborhood density (i.e., density of neighboring live trees at the start of the outbreak). Our results suggest a tradeoff in the role of pre-disturbance suppression on post-disturbance compensatory response. While small-diameter trees, those most likely to be suppressed, demonstrated the strongest responses to neighborhood mortality, trees experiencing high levels of pre-outbreak suppression may have had a reduced capacity for recovery once resource availability increased. This is potentially due to physiological effects of suppression (Wright et al. 2000) or persistent impacts of standing dead trees, which can impede growth by continuing to shade surviving trees or inflicting injury via falling branches (Dhar and Hawkins 2011). Interestingly, we found no evidence that growth releases of Engelmann spruce decreased with initial neighborhood density, suggesting this species may be more capable of persisting through and recovering from suppression once resources are released (Andrus et al. 2018). Our results for lodgepole pine (a shade-intolerant species) and Engelmann spruce (a shade-tolerant species) support the idea that growth releases of shade-intolerant species are more negatively impacted by the level of suppression prior to resource release than shade-tolerant species (Wright et al. 2000). These size- and species-specific differences in how individual trees responded to neighborhood structure and mortality have important implications for dendroecological reconstructions of historical bark beetle outbreaks (e.g., Negrón and Huckaby 2020), as both the size of the tree at the time of an outbreak as well as its location relative to other trees in a stand will impact the ability to detect a historical outbreak (Thompson et al. 2007).

While our study focused on growth responses, our findings also demonstrate the role of pre-outbreak stand structure and outbreak severity in dictating post-outbreak successional dynamics (Diskin et al. 2011; Morris et al. 2022). When combined, selective mortality of the overstory and growth release of the understory often accelerate the succession of stands towards late-seral, shade-tolerant species (Cole and Amman 1980; Heath and Alfaro 1990). Our finding that late-seral species (i.e., Engelmann spruce and subalpine fir) had the highest growth responses, and that aggregate BA growth and overstory recruitment were highest in areas dominated by late-seral species, suggests our study plots will trend toward dominance by late-seral species following the outbreak, as found elsewhere within our study region (Collins et al. 2011, 2012). Lodgepole pine will remain an important component of our study stands, however, as it continued to dominate post-outbreak overstory recruitment (i.e., total number of stems). These findings highlight how pre-outbreak spatial pattern acts as a persistent biological legacy shaping post-outbreak stand development dynamics (Bače et al. 2015), which in turn will shape how these stands respond to future disturbance (Turner et al. 2013).

Spatial patterns of aggregate growth emerge from the growth and spatial arrangement of individual trees

Across the within-stand landscape, aggregate growth responses were driven and constrained by spatial legacies of the outbreak: the growth responses and spatial arrangement of individual survivors. Fine-scale heterogeneity in neighborhood density and mortality led to a wide range of individual tree growth responses. Emergent patterns of aggregate BA growth and overstory recruitment, which also varied widely within stands, follow from this variation in growth responses of individual trees. For example, our finding that aggregate BA growth and overstory recruitment were highest in neighborhoods dominated by late-seral species follows from the greater growth responses of late-seral species relative to lodgepole pine. Similarly, our finding that aggregate overstory recruitment density increased with neighborhood mortality follows from the strong compensatory responses of small-diameter trees. However, while resources released by mortality may increase growth at the tree level for individual survivors, aggregate within-stand growth is strongly determined by the number and size of trees that survive. Post-outbreak aggregate BA growth rates and releases decreased with neighborhood mortality, likely because overstory mortality reduces

surviving BA and stem density, thereby reducing the aggregate potential for BA growth (Long and Vacchiano 2014). These results illustrate the limits on aggregate population-level compensatory responses imposed by the number, size, and spatial arrangement of survivors. These results also illustrate the role of within-stand spatial heterogeneity in shaping compensatory growth responses across scales.

Drivers and spatial patterns of aggregate growth shifted from pre- to post-outbreak as overstory mortality altered the growth responses of individual survivors. Prior to the outbreak, for example, aggregate BA growth rates were highest in neighborhoods with larger trees (i.e., after accounting for stem density, aggregate BA growth increased with BA). Following the outbreak, however, neighborhoods composed of small trees yielded levels of aggregate BA growth comparable to neighborhoods composed of the same number of large trees. From pre- to post-outbreak, the relative magnitude of drivers of overstory recruitment also shifted, with fine-scale topography playing a stronger role in the pre-outbreak period compared to the post-outbreak period, when overstory recruitment was related primarily to late-seral proportion and neighborhood mortality. These shifts in drivers of aggregate growth metrics contributed to qualitative shifts in the spatial patterns of BA growth and overstory recruitment from pre- to post-outbreak. Thus, not only did the outbreak alter stand structure directly, redistributing biomass within the stand (Donato et al. 2013; Morris et al. 2022); it also redistributed within-stand patterns of productivity (Romme et al. 1986).

Conclusion

Compensatory responses of forests, wherein the loss of one forest component is compensated for by the growth of another following disturbance, are key mechanisms of resilience with strong stabilizing effects within forest communities (Gonzalez and Loreau 2009). Overall, we found strong evidence for compensatory responses across spatial scales. Overstory recruitment density increased as growth releases of small-diameter trees accelerated growth of understory trees into the overstory. Despite net decreases in live BA caused by the outbreak, increases in growth rates of surviving trees were sufficient to maintain stability in rates of biomass accumulation within our study stands. Our findings illustrate how compensatory responses of individual trees vary widely with size, species, and spatial position within a stand, demonstrating the importance of spatially explicit, individual-based modeling approaches for reconstructing spatial patterns of historical disturbance (Vašíčková et al. 2019) and predicting post-disturbance forest dynamics (Seidl et al. 2012). Post-outbreak growth rates and growth releases were greatest for small-diameter trees located in neighborhoods with high levels of overstory mortality, with late-seral, shade-tolerant species exhibiting the greatest growth responses both prior to and following the outbreak. This variation in individual tree responses, combined with the spatial pattern of surviving trees, resulted in highly variable emergent patterns of aggregate BA growth and overstory recruitment. Quantifying the ways in which forests compensate for stand-releasing disturbances such as bark beetle outbreaks is critical for modeling post-disturbance stand development and forest carbon dynamics (Dhar and Hawkins 2011; Pfeifer et al. 2011). By evaluating forest compensatory responses in a spatially explicit framework, our findings highlight the role of landscape composition and configuration in shaping forest resilience (Chambers et al. 2019).

Acknowledgements We thank the USDA Forest Service Rocky Mountain Research Station, K. Elder, B. Starr, and D. McClain for facilitating access to field sites and housing in the Fraser Experimental Forest. We thank F. Carroll, N. Lau, A. Link, A. Liu, S. Riedel, and R. T. Sternberg for field assistance and E. Vilanova for FieldMap training. This work would not have been possible without the 1989 and 2004 surveys led by J. Franklin, W. Moir, and M. Harmon; we are extraordinarily grateful for the meticulous data collection of their field crews and for the data curation of R. Pabst. We are grateful for insight provided by J. Negrón and C. Rhoades, and for feedback provided by T. Veblen and one anonymous reviewer.

Author contributions MSB and BJH conceived and designed the study, with input from all authors. All authors were involved with field data collection. MSB led data analysis with guidance from BJH and input from all authors. MSB and BJH wrote the manuscript, and all authors contributed critically to drafts and approved the final manuscript.

Funding This work was supported by the McIntire-Stennis Cooperative Forestry Research Program (grant no. NI17MSC-FRXXXG003/project accession no. 1012773) from the USDA National Institute of Food and Agriculture and by the National Science Foundation (DEB 1853520). Additional funding was provided by the School of Environmental and Forest Sciences,

the Quantitative Ecology and Resource Management Program, and the Student Technology Fee at the University of Washington. BJ Harvey acknowledges support from the Jack Corkery and George Corkery Jr. Endowed Professorship in Forest Sciences.

Data availability Datasets analyzed in this study are available on Zenodo: https://doi.org/10.5281/zenodo.7314248

Declarations

Conflict of interest The authors have no relevant interests to disclose.

References

Andrus RA, Harvey BJ, Chai RK, Veblen TT (2018) Different vital rates of engelmann spruce and subalpine fir explain discordance in understory and overstory dominance. Can J For Res 48:1554–1562.

Astrup R, Coates KD, Hall E (2008) Recruitment limitation in forests: lessons from an unprecedented mountain pine beetle epidemic. For Ecol Manag 256:1743–1750.

Axelson JN, Alfaro RI, Hawkes BC (2009) Influence of fire and mountain pine beetle on the dynamics of lodgepole pine stands in British Columbia, Canada. For Ecol Manag 257:1874–1882.

Bače R, Svoboda M, Janda P et al (2015) Legacy of pre-disturbance spatial pattern determines early structural diversity following severe disturbance in montane spruce forests. PLoS ONE 10:1–18

Bradford JB, Birdsey RA, Joyce LA, Ryan MG (2008) Tree age, disturbance history, and carbon stocks and fluxes in subalpine rocky Mountain forests. Glob Change Biol 14:2882–2897

Brown MG, Black TA, Nesic Z et al (2012) The carbon balance of two lodgepole pine stands recovering from mountain pine beetle attack in British Columbia. Agric For Meteorol 153:82–93

Buonanduci MS, Morris JE, Agne MC, Harvey BJ (2020) Neighborhood context mediates probability of host tree mortality in a severe bark beetle outbreak. Ecosphere 11:e03236

Caspersen JP, Vanderwel MC, Cole WG, Purves DW (2011) How stand productivity results from size- and competition-dependent growth and mortality. PLoS ONE.

Chai RK, Andrus RA, Rodman K et al (2019) Stand dynamics and topographic setting influence changes in live tree biomass over a 34-year permanent plot record in a subalpine forest in the Colorado front range. Can J For Res 49:1256–1264

Chambers JC, Allen CR, Cushman SA (2019) Operationalizing ecological resilience concepts for managing species and ecosystems at risk. Front Ecol Evol 7:1–27

Chapman TB, Veblen TT, Schoennagel T (2012) Spatiotemporal patterns of mountain pine beetle activity in the southern rocky mountains. Ecology 93:2175–2185

Chesson P (2000) Mechanisms of maintenance of species diversity. Annu Rev Ecol Syst 31:343–366

Collins BJ, Rhoades CC, Hubbard RM, Battaglia MA (2011) Tree regeneration and future stand development after bark beetle infestation and harvesting in Colorado lodgepole pine stands. For Ecol Manag 261:2168–2175

Collins BJ, Rhoades CC, Battaglia MA, Hubbard RM (2012) The effects of bark beetle outbreaks on forest development, fuel loads and potential fire behavior in salvage logged and untreated lodgepole pine forests. For Ecol Manag 284:260–268

Contreras MA, Affleck D, Chung W (2011) Evaluating tree competition indices as predictors of basal area increment in western Montana forests. For Ecol Manag 262:1939–1949

Craine JM, Dybzinski R (2013) Mechanisms of plant competition for nutrients, water and light. Funct Ecol 27:833–840

Cumming GS (2011) Spatial resilience: integrating landscape ecology, resilience, and sustainability. Landsc Ecol 26:899–909

Dale VH, Joyce LA, McNulty S et al (2001) Climate change and forest disturbances. Bioscience 51:723–734

Davis TS, Meddens AJH, Stevens-Rumann CS, Jansen VS, Sibold JS, Battaglia MA (2022) Monitoring resistance and resilience using carbon trajectories: Analysis of forest management-disturbance interactions. Ecol Appl. e2704

DeRose RJ, Long JN (2010) Regeneration response and seedling bank dynamics on a Dendroctonus rufipennis-killed Picea engelmannii landscape. J Veg Sci 21:377–387

Dhar A, Hawkins CDB (2011) Regeneration and growth following mountain pine beetle attack: a synthesis of knowledge. BC J Ecosyst Manag 12:1–16

Diskin M, Rocca ME, Nelson KN et al (2011) Forest developmental trajectories in mountain pine beetle disturbed forests of rocky mountain national park, Colorado. Can J For Res 41:782–792

Donato DC, Harvey BJ, Romme WH et al (2013) Bark beetle effects on fuel profiles across a range of stand structures in douglas-fir forests of greater yellowstone. Ecol Appl 23:3–20.

Franklin JF, Lindenmayer D, Macmahon JA et al (2000) Threads of continuity: ecosystem disturbance, recovery, and the theory of biological legacies. Conserv Pract 1:8–17

Franklin JF, Spies TA, Van Pelt R et al (2002) Disturbances and structural development of natural forest ecosystems with silvicultural implications, using Douglas-fir forests as an example. For Ecol Manag 155:399–423

Fuglstad GA, Simpson D, Lindgren F, Rue H (2018) Constructing priors that penalize the complexity of gaussian random fields. J Am Stat Assoc 1459:1–8.

Getzin S, Dean C, He F et al (2006) Spatial patterns and competition of tree species in a Douglas-fir chronosequence on Vancouver Island. Ecography 29:671–682

Gonzalez A, Loreau M (2009) The causes and consequences of compensatory dynamics in ecological communities. Annu Rev Ecol Evol Syst 40:393–414.

Griesbauer H, Green S (2006) Examining the utility of advance regeneration for reforestation and timber production in unsalvaged stands killed by the mountain pine beetle: controlling factors and management implications. BC J Ecosyst Manag 7:81–92

Hawkins CDB, Dhar A, Balliet NA (2013) Radial growth of residual overstory trees and understory saplings after mountain pine beetle attack in central British Columbia. For Ecol Manag 310:348–356

Heath R, Alfaro RI (1990) Growth response in a Douglas-fir/lodgepole pine stand after thinning of lodgepole pine by the mountain pine beetle: a case study. J Entomol Soc Br Columbia 87:16–21

Holling CS (1973) Resilience and stability of ecological systems. Annu Rev Ecol Syst 4:1–23

Hubbard RM, Rhoades CC, Elder K, Negrón JF (2013) Changes in transpiration and foliage growth in lodgepole pine trees following mountain pine beetle attack and mechanical girdling. For Ecol Manag 289:312–317

Huckaby LS, Moir WH (1998) Forest communities at fraser experimental forest, Colorado. Southwest Nat 43:204–218

Jarvis DS, Kulakowski D (2015) Long-term history and synchrony of mountain pine beetle outbreaks in lodgepole pine forests. J Biogeogr 42:1029–1039

Lindgren F, Rue H, Lindström J (2011) An explicit link between Gaussian fields and Gaussian Markov random fields: the stochastic partial differential equation approach. J Royal Stat Society: Ser B (Statistical Methodology) 73:423–498

Long JN, Vacchiano G (2014) A comprehensive framework of forest stand property-density relationships: perspectives for plant population ecology and forest management. Ann For Sci 71:325–335.

Long JN, Dean TJ, Roberts SD (2004) Linkages between silviculture and ecology: examination of several important conceptual models. For Ecol Manag 200:249–261.

Lutz JA, Larson AJ, Furniss TJ et al (2014) Spatially nonrandom tree mortality and ingrowth maintain equilibrium pattern in an old-growth Pseudotsuga–Tsuga forest. Ecology 95:2047–2054

Meddens AJH, Hicke JA, Ferguson CA (2012) Spatiotemporal patterns of observed bark beetle-caused tree mortality in British Columbia and the western United States. Ecol Appl 22:1876–1891

Morris JE, Buonanduci MS, Agne MC et al (2022) Does the legacy of historical thinning treatments foster resilience to bark beetle outbreaks in subalpine forests? Ecol Appl 32:e02474

Negrón JF, Huckaby L (2020) Reconstructing historical outbreaks of mountain pine beetle in lodgepole pine forests in the Colorado Front Range. For Ecol Manag 473:118270

Nigh GD, Antos JA, Parish R (2010) Density and distribution of advance regeneration in mountain pine beetle killed lodgepole pine stands of the Montane Spruce zone of southern British Columbia. Can J For Res 38:2826–2836

Pettit LI (1990) The conditional predictive ordinate for the normal distribution. J Roy Stat Soc: Ser B (Methodol) 52:175–184

Pfeifer EM, Hicke JA, Meddens AJH (2011) Observations and modeling of aboveground tree carbon stocks and fluxes following a bark beetle outbreak in the western United States. Glob Change Biol 17:339–350

Porté A, Bartelink HH (2002) Modelling mixed forest growth: a review of models for forest management. Ecol Model 150:141–188

Pukkala T, Lähde E, Laiho O (2009) Growth and yield models for uneven-sized forest stands in Finland. For Ecol Manag 258:207–216

R Core Team (2021) R: a language and environment for statistical computing. R Foundation for Statistical Computing, Vienna, Austria

Rhoades CC, Hubbard RM, Elder K (2017) A decade of streamwater nitrogen and forest dynamics after a mountain pine beetle outbreak at the fraser experimental forest, Colorado. Ecosystems 20:380–392

Rodman KC, Andrus RA, Carlson AR et al (2022) Rocky mountain forests are poised to recover following bark beetle outbreaks but with altered composition. J Ecol.

Romme WH, Knight DH, Yavitt JB (1986) Mountain pine beetle outbreaks in the rocky mountains: regulators of primary productivity? Am Nat 127:484–494

Rouvinen S, Kuuluvainen T (1997) Structure and asymmetry of tree crowns in relation to local competition in a natural mature Scots pine forest. Can J For Res 27:890–902

Seidl R, Rammer W, Scheller RM, Spies TA (2012) An individual-based process model to simulate landscape-scale forest ecosystem dynamics. Ecol Model 231:87–100

Simard M, Powell EN, Raffa KF, Turner MG (2012) What explains landscape patterns of tree mortality caused by bark beetle outbreaks in Greater Yellowstone? Glob Ecol Biogeogr 21:556–567

Thompson RD, Daniels LD, Lewis KJ (2007) A new dendroecological method to differentiate growth responses to fine-scale disturbance from regional-scale environmental variation. Can J For Res 37:1034–1043

Thorpe HC, Astrup R, Trowbridge A, Coates KD (2010) Competition and tree crowns: a neighborhood analysis of three boreal tree species. For Ecol Manag 259:1586–1596

Turner MG (2010) Disturbance and landscape dynamics in a changing world. Ecology 91:2833–2849

Turner MG, Donato DC, Romme WH (2013) Consequences of spatial heterogeneity for ecosystem services in changing forest landscapes: priorities for future research. Landscape Ecol 28:1081–1097

van Lierop P, Lindquist E, Sathyapala S, Franceschini G (2015) Global forest area disturbance from fire, insect pests, diseases and severe weather events. For Ecol Manag 352:78–88

Vašíčková I, Šamonil P, Král K et al (2019) Driving factors of the growth response of *Fagus sylvatica* L. to disturbances: a comprehensive study from Central-European old-growth forests. For Ecol Manag 444:96–106

Veblen TT, Hadley KS, Reid MS, Rebertus AJ (1991) The response of subalpine forests to spruce beetle outbreak in Colorado. Ecology 72:213–231

Vorster AG, Evangelista PH, Stohlgren TJ et al (2017) Severity of a mountain pine beetle outbreak across a range of stand conditions in fraser experimental forest, Colorado, United States. For Ecol Manag 389:116–126

Weiner J, Thomas SC (2001) The nature of tree growth and the "age-related decline in forest productivity". Oikos 94:374–376

Wild J, Kopecký M, Svoboda M et al (2014) Spatial patterns with memory: tree regeneration after stand-replacing disturbance in *Picea abies* mountain forests. J Veg Sci 25:1327–1340

Woodall CW, Fiedler CE, Milner KS (2003) Intertree competition in uneven-aged ponderosa pine stands. Can J For Res 33:1719–1726

Wright EF, Canham CD, Coates KD (2000) Effects of suppression and release on sapling growth for 11 tree species of northern, interior British Columbia. Can J For Res 30:1571–1580

Alfaro RI, Campbell R, Vera P, et al. (2003) Dendroecological reconstruction of mountain pine beetle outbreaks in the Chilcotin Plateau of British Columbia. Mountain Pine Beetle Symposium: Challenges and Solutions 245–256

Blangiardo M, Cameletti M (2015) Spatial and spatio-temporal Bayesian models with R-INLA. John Wiley & Sons

Cliff AD, Ord JK (1981) Spatial processes: models & applications. Taylor & Francis

Cole WE, Amman GD (1980) Mountain pine beetle dynamics in lodgepole pine forests, Part I: Course of an infestation. USDA Forest Service, Intermountain Forest and Range Experiment Station, General Technical Report *INT-188*

Hawkes BC, Taylor SW, Stockdale C et al (2003) Impact of mountain pine beetle on stand dynamics in British Columbia. Mountain Pine Beetle Symposium: Challenges and Solutions 177–199

Hédl R, Svátek M, Dančák M et al (2009) A new technique for inventory of permanent plots in tropical forests: A case study from lowland dipterocarp forest in Kuala Belalong, Brunei darussalam. Blumea: Journal of Plant Taxonomy and Plant Geography 54:124–130

Krainski ET, Gómez-Rubio V, Bakka H et al (2019) Advanced Spatial Modeling with Stochastic Partial Differential Equations Using R and INLA. Chapman & Hall/CRC Press

Pickett ST, White PS (1985) The ecology of natural disturbance and patch dynamics. Academic Press

PRISM Climate Group (2021) PRISM Gridded Climate Data Oregon State University https://prism.oregonstate.edu

Tishmack J, Mata SA, Schmid JM (2005) Mountain pine beetle emergence from lodgepole pine at different elevations near Fraser, CO. Research Note RMRS-RN-27. Fort Collins, CO: US Department of Agriculture, Forest Service, Rocky Mountain Research Station *27 RMRS-RN*1–5

Weiss A (2001) Topographic position and landforms analysis. Poster Presentation, ESRI User Conference, San Diego, CA

Wilm H, Dunford E(1948) Effect of timber cutting on water available for stream flow from a lodgepole pine forest. USDA Technical Bulletin *968*1–43